First publ. in: Molecular Physics 100 (2002), 9, pp. 1413-1420

Solvent effects on the intrinsic enhancement factors of the triplet exciplex generated by photoinduced electron transfer reaction between eosin Y and duroquinone

TAKASHI TACHIKAWA[1], YASUHIRO KOBORI[1], KIMIO AKIYAMA[1], AKIO KATSUKI[2], YOSHIHARU USUI[3], ULRICH E. STEINER[4] and SHOZO TERO-KUBOTA[1]*

[1] Institute of Multidisplinary Research for Advanced Materials, Tohoku University, Sendai, 980-8577, Japan

[2] Department of Chemistry, Faculty of Education, Shinshu University, Nagano, 389-5144, Japan

[3] Department of Environmental Sciences, Faculty of Science, Ibaraki University, Mito 310-8512, Japan

[4] Fachbereich Chemie, University of Konstanz, D-78457 Konstanz, Germany

The spin dynamics of the duroquinone anion radical ($DQ^{\cdot -}$) generated by photoinduced electron transfer reactions from triplet eosin Y ($^3EY^{2-}$) to DQ have been studied by using transient absorption and pulsed EPR spectroscopy. Unusual net-absorptive electron spin polarization plus net-emissive polarization were observed, suggesting the production of the triplet exciplex or contact radical pair as the reaction intermediate. The kinetic parameters and intrinsic enhancement factors of the electron spin polarization were determined in various alcoholic solvents. The net-absorptive electron spin polarization was also observed in ethanol–water mixed solvents. The solvent effects on the radical yield are analysed on the basis of a stochastic Liouville equation established for the magnetic field effects on the radical yield. The zero-field splitting constants of the triplet exciplex are estimated from the solvent viscosity dependence of the enhancement factors due to spin–orbit coupling induced depopulation of the reaction intermediate.

1. Introduction

There has been considerable interest in exciplexes or contact radical pairs in photoinduced electron transfer reactions because they are important intermediates in photochemistry. Short range interactions such as spin–orbit coupling (SOC) operate in exciplexes [1–6]. Steiner *et al.* [2, 7–11] found remarkable magnetic field effects on the radical yield in the photoinduced electron transfer reaction between thionine and halogenated anilines in polar solvents. The effect was interpreted in terms of the sublevel selective back electron transfer reaction due to the SOC from the triplet exciplex to the ground state. The chemically induced dynamic electron polarization (CIDEP) spectra also give valuable information about these reaction intermediates and their dynamics. The unusual net-absorptive (net-A) CIDEP spectra observed in several photoinduced electron transfer reactions containing heavy atoms verified the generation of the triplet exciplex as the intermediate [5, 6, 12–17]. It has been concluded that the net-A CIDEP results from the sublevel selective back electron transfer from the triplet exciplex to the ground singlet state due to SOC. Recently, Steiner and coworkers [18, 19] performed a unified study of the magnetic field effects and electron spin polarizaton due to SOC selective populations into the triplet precusor (p-type triplet mechanism, or p-TM) and depopulation of triplet sublevels from the triplet exciplex (d-type triplet mechanism or d-TM) on the basis of the stochastic Liouville equation. The triplet exciplexes are considered to have a cofacial sandwich-type structure as suggested by Kochi [20–22].

Observation of the normal radical pair mechanism (RPM) suggests a negligibly small energy difference between the singlet and triplet states of the radical pairs, indicating the production of solvent-separated

* Author for correspondence. e-mail: tero@tagen.tohoku.ac.jp

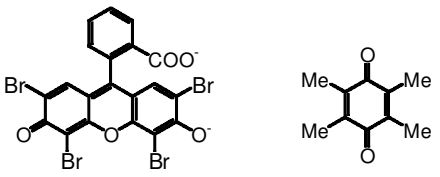

Eosin Y (EY^{2-}) Duroquinone (DQ)

Figure 1. Structures of the donor and acceptor.

radical pairs as intermediates [23, 24]. The triplet mechanism gives proof of the triplet precursor reactions [25, 26]. The cleavage reaction of the triplet state was also clarified by observation of the d-TM in alkyl radical formation from azoalkanes [27, 28]. On the other hand, the unusual net-A CIDEP generated by a bimolecular process verifies the production of exciplexes, since SOC is a short range interaction. It is expected that the intrinsic enhancement factors of the CIDEP spectra provide information about the dynamics and molecular interactions of the short lived species. However, there have been few studies of the intrinsic enhancement factors in triplet exciplex formation systems. For the duroquinone (DQ) plus 4-halogen-*N*,*N*-dimethylaniline derivative systems we have determined the intrinsic enhancement factor of the electron spin polarization [16]. Significant solvent effects on the electron spin polarization and magnetic field effects on the radical yield were obtained [16, 17]. In methanol, the $S–T_0$ mixing due to the normal RPM was observed clearly, suggesting the formation of solvent separated radical ion pairs. On the other hand, in 1-propanol and 1-butanol it has been verified that SOC due to the heavy atoms governs the spin polarization and radical yields, suggesting that a triplet exciplex or contact radical ion pair is a key intermediate. For the photoinduced electron transfer reaction betwen xanthene dyes and quinones we have reported that the apparent enhancement factor of the electron spin polarization increases with increasing atomic number of the halogen substituents [13, 14].

In the present study we have determined the intrinsic enhancement factors of the electron spin polarization for the eosin Y–DQ system by analysing the time profiles of the echo-detected FT-EPR spectra in several alcoholic solvents. Eosin Y is a useful photoreductive sensitizer for examining SOC effects on spin dynamics, because it has heavy atoms as shown in figure 1 [29]. The transient absorption spectra were measured to determine the escape radical yields from the solvent cage. We shall discuss the mechanism and dynamics of the electron spin polarization based on the solvent dependence of the enhancement factors and the escape radical yield.

2. Experimental

Eosin Y (2′,4′,5′,7′-tetrabromo-3′,6′-dihydroxyspiro-[isobenzofuran-1(3*H*),9′-[9*H*]xanthen]-3-one disodium salt, EY^{2-}) was purchased from Nacalai Tesque and was recrystallized from ethanol. DQ (Tokyo Kasei) was purified by vacuum sublimation in the dark. Methanol (MeOH, reagent grade), ethanol (EtOH, spectrograde), 1-propanol (1-PrOH) and 1-butanol (1-BuOH) were purchased from Nacalai Tesaque and were used as solvents without further purification.

Nanosecond transient absorption spectra were measured by using a multichannel analyser (diode array, Princeton Instruments IRY-700) controlled with a personal computer as described previously [16]. A Holographic Notch-plus^{TM} filter (Kaiser Optical System HNPF-532) was used to protect the detector from the strong laser light. The transient signals were recorded with a digitizer (Tektronix TDS 520D).

Echo detected FT-EPR measurements were performed by using an X band pulsed EPR spectrometer (Bruker ESP 380E) equipped with a dielectric resonator ($Q \sim 100$). The methods for the electron spin–echo detection and phase correction have been described elsewhere [15]. A microwave pulse width of 16 ns was used for a $\pi/2$ pulse.

All sample solutions were deoxygenated by argon gas bubbling and allowed to flow into a quartz cell within a laser photolysis spectrometer or an EPR resonator. In the present study, EY^{2-} was selectively excited by an Nd:YAG laser (Spectra-Physics GCR-155, INDI-40-20, 532 nm). All measurements were performed at room temperature.

3. Results and discussion

3.1. *Escape radical yields*

Figure 2 shows the transient absorption spectra obtained by laser photolysis of EY^{2-} (5×10^{-5} mol dm^{-3}) with 532 nm light in the presence of DQ (1×10^{-3} mol dm^{-3}) in EtOH. The transient spectra represent averages of 256 signals. The transient absorption band at 560–700 nm appears immediately after the laser pulse. The absorption band is attributable to triplet EY^{2-}($^3EY^{2-}$) [30–34]. The bleaching in the 480–550 nm region is due to the absorption of ground state EY^{2-}. The decay of the T–T absorption was accompanied by the concomitant growth of the absorption with a peak maximum at 445 nm. The change in the transient absorption spectra in figure 2 suggests electron transfer from $^3EY^{2-}$ to DQ (scheme 1). Although the generation of the triplet exciplex or contact radical pair is unclear from the present transient absorption spectra, the short lived intermediate may be verified by the CIDEP experiments as discussed later. Heavy atom substituents induce sublevel selective intersystem crossing (ISC)

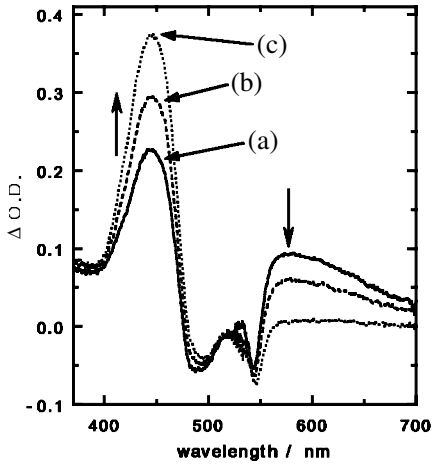

Figure 2. Transient absorption spectra obtained by laser photolysis of EY^{2-} (5×10^{-5} mol dm^{-3}) with 532 nm light in the presence of DQ (1×10^{-3} mol dm^{-3}) in EtOH. The measurements were performed at 0.2 μs (a), 0.4 μs (b), and 2.0 μs (c), with the gate width of 0.1 μs after the laser pulse.

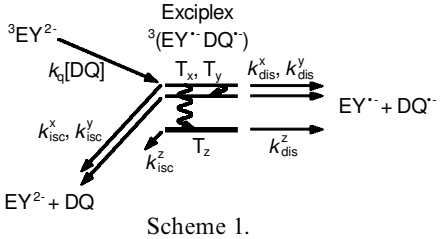

Scheme 1.

from the triplet exciplex into the ground state, although the dissociation of the exciplex is non-selective [2, 7–9, 13]. The escape yield of the free radicals from the solvent cage is described as follows:

$$\phi_{esc} = \left(1 + \frac{\sum k^i_{isc}}{\sum k^i_{dis}}\right)^{-1}, \qquad (1)$$

where k^i_{isc} and k^i_{dis} ($i = x, y, z$) denote the rate constants of the ISC and dissociation of the triplet exciplex, respectively.

The transient absorption spectrum observed 2 μs after the laser pulse can be attributed to the superimposed absorption bands of $EY^{\cdot -}$ and $DQ^{\cdot -}$. This assignment is confirmed by the quenching reaction of $EY^{\cdot -}$ by triethanolamine (TEOA) [34, 35]:

$$EY^{\cdot -} + TEOA \rightleftarrows EY^{2-} + TEOA^{\cdot +} \qquad (2)$$

As shown in figure 3 spectrum b, a transient absorption with a peak maximum at 440 nm with a shoulder at 420 nm was observed by the laser photolysis of EY^{2-} in the presence of DQ and triethanolamine (1×10^{-2} mol dm^{-3}) in EtOH. The spectrum is attributed to $DQ^{\cdot -}$ [16, 36]. The absorption spectrum obtained by the subtraction of spectrum b from spectrum a in

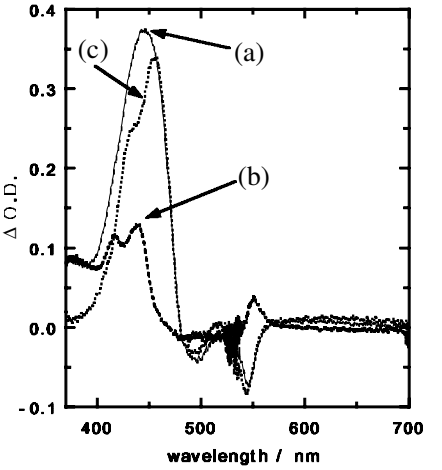

Figure 3. Transient absorption spectra obtained by laser photolysis with 532 nm of EY^{2-} (5×10^{-5} mol dm^{-3}) in the presence of DQ (1×10^{-3} mol dm^{-3}) (a) and DQ (1×10^{-3} mol dm^{-3}) and triethanolamine (1×10^{-2} mol dm^{-3}) (b) in EtOH. The measurements were performed at 2.0 μs (a) and 50 μs (b) after the laser pulse. Spectrum c is obtained from the subtraction of b from a.

figure 3 corresponds to that of $EY^{\cdot -}$ [30–34]. The present result suggests that peak maximum (457 nm) of the $EY^{\cdot -}$ absorption band is not overlapped by the band due to $DQ^{\cdot -}$. Therefore, the ϕ_{esc} values were determined using the ratio of the change in optical density of $EY^{\cdot -}$ ($\varepsilon(462\,nm) = 60\,000$ mol^{-1} dm^3 cm^{-1}) [30] and $^3EY^{2-}$ ($\varepsilon(580\,nm) = 9400$ mol^{-1} dm^3 cm^{-1}) [31]. A ϕ_{esc} value of 0.54 was obtained in EtOH. The measurements of the transient absorption spectra were also performed in several alcohol solvents, and values of 0.58, 0.45 and 0.39 were obtained in MeOH, 1-PrOH and 1-BuOH, respectively.

Figure 4 shows the time profiles of the transient absorption signals at 440 nm observed by the laser

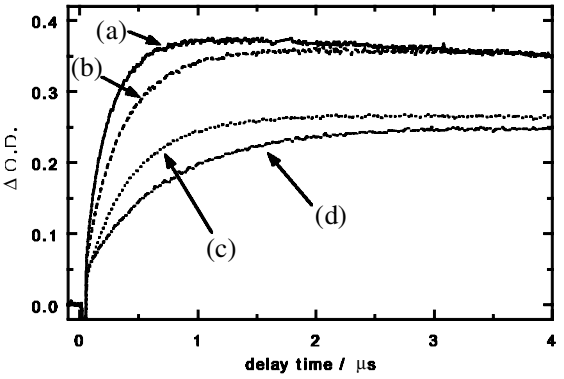

Figure 4. Growth time profiles of the transient absorption band at 440 nm obtained by laser photolysis of EY^{2-} (5×10^{-5} mol dm^{-3}) in the presence of DQ (1×10^{-3} mol dm^{-3}) iin MeOH (a), EtOH (b), 1-PrOH (c) and 1-BuOH (d).

Table 1. Kinetic parameters and intrinsic enhancement factors of $DQ^{\cdot -}$ generated by the photoinduced electron transfer from EY^{2-} in several alcohols as determined from transient absorption and FT-EPR spectroscopy.

Solvent (η/ m Pa s; ε)	ϕ_{esc}	$k_q/10^9\,M^{-1}\,s^{-1}$	T_1^T/ns	T_1^R/μs	V_{pd}	V_d
MeOH (0.545; 32.6)	0.58	(5.2)[a] 5.5[b]	9	0.6	−32 (±4)	8 (±2)
EtOH (1.10; 24.4)	0.54	(3.1) 2.8	10	0.8	−40 (±4)	11.5 (±2)
1-PrOH (1.97; 20.3)	0.45	(2.5) 2.7	10	0.9	−44 (±4)	14 (±1)
1-BuOH (2.61; 17.5)	0.39	(1.3) 1.4	11	0.9	−52 (±4)	16 (±2)

[a] Determined from the transient absorption experiments.
[b] Determined from the FT-EPR experiments.

photolysis of the EY^{2-} $(5\times10^{-5}\,mol\,dm^{-3})-DQ$ $(1\times10^{-3}\,mol\,dm^{-3})$ system in several alcohols. Assuming a pseudo-first-order reaction, the quenching rate constants k_q were determined, values are summarized in table 1. These k_q are slightly smaller than the diffusion-controlled rate constants.

3.2. *Time profiles of the FT-EPR signals*

Figure 5 depicts the evolution and decay of the echo-detected FT-EPR signals due to the DQ anion radical ($DQ^{\cdot -}$, $a^H = 0.19$ mT and $g = 2.0041$) generated by laser photolysis of the EY^{2-}-DQ system in 1-PrOH at room temperature. The measurements were performed for an EY^{2-} concentration of $1\times10^{-4}\,mol\,dm^{-3}$ and the DQ concentrations of $4\times10^{-3}\,mol\,dm^{-3}$ (curve a), $1\times10^{-3}\,mol\,dm^{-3}$ (curve b) and $1\times10^{-4}\,mol\,dm^{-3}$ (curve c) in 1-PrOH. When the DQ concentration was higher than $1\times10^{-3}\,mol\,dm^{-3}$, the net-E CIDEP spectra due to the triplet mechanism were observed during the early time ($t \le 60$ ns) as shown in the inset spectrum a′ in figure 5. Subsequently, the net-A CIDEP signals appeared (inset spectrum a″ in figure 5). The net-A signals are attributable to SOC induced depopulation from the triplet sublevels of the exciplex (d-TM), because remarkable heavy atom effects on the enhancement factor have been observed in the xanthene dye-sensitized reduction of DQ [13, 14]. By contrast, the net-E CIDEP is negligible in the low concentrations of the acceptor, DQ, as shown in figure 5, curve c. The buildup rate of the net-A CIDEP signals depends significantly on the DQ concentration, suggesting that the net-A polarization is created during a bimolecular process. The solid lines are obtained from the nonlinear least-squares fits based on the modified Bloch equation (discussed later). Observation of the net-A polarization due to the d-TM suggests the production of the triplet exciplex as the reaction intermediate, because SOC due to heavy atoms is short range. The intermediate would be a nearly pure charge transfer complex or contact radical pair in the polar solvent.

Scheme 2 shows the net electron spin polarization mechanism from the spin polarized and spin equilibrated triplet precursor via the triplet exciplex in the present photosensitized reaction. The photoinduced electron transfer occurs dominantly from the excited triplet states of EY^{2-} because of the fast ISC. This is supported by the observation of the net-E TM in the early time. The relaxation process of the spin polarized

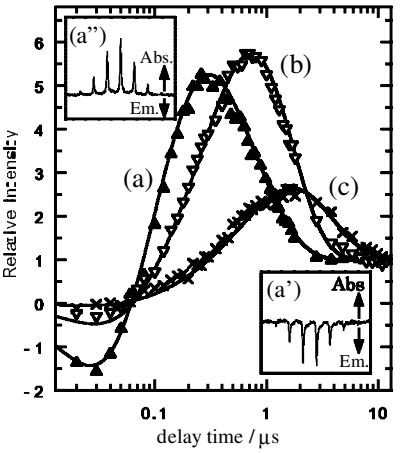

Figure 5. Acceptor concentration dependence of the time profiles of the echo FT-EPR signals due to $DQ^{\cdot -}$ generated from the laser photo-excitation of EY^{2-} in the presence of DQ in 1-PrOH. The measurements were carried out with the concentrations of $[EY^{2-}] = 1\times10^{-4}\,mol\,dm^{-3}$, $[DQ] = 4\times10^{-3}\,mol\,dm^{-3}$ (a), $1\times10^{-3}\,mol\,dm^{-3}$ (b) and $1\times10^{-4}\,mol\,dm^{-3}$ (c). Insets: echo FT-EPR spectra observed in the EY-DQ $(4\times10^{-3}\,mol\,dm^{-3})$ system at the delay time of 30 ns (a') and 100 ns (a''). The solid lines represent nonlinear least-squares curve fits based on the data shown in table 1.

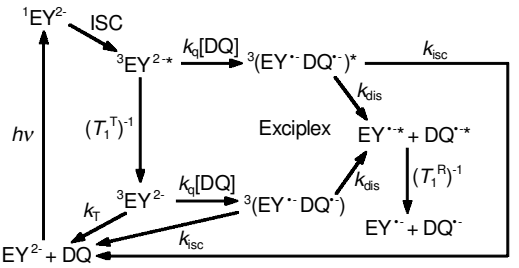

Scheme 2.

triplet state (triplet relaxation time T_1^T) competes with the quenching reaction, k_q [DQ]. The net-A CIDEP signals are attributable to the sublevel selective back electron transfer, which produces the ground singlet state directly. According to scheme 2, we obtain the magnetization on the radicals based on the Bloch equations as follows:

$$\frac{dM_z}{dt} = k_q[DQ]\phi_{esc}P_d C_T + k_q[DQ]\phi_{esc}P_{dp}C_{T^*} - \frac{M_z - \phi_{esc}(t)P_{eq}}{T_1^R}, \quad (3)$$

where the first term corresponds to the net-A polarization due to the d-TM with polarization P_d, the second term is the contribution from the concomitant d-TM and p-TM with polarization P_{dp}, and the last term represents the dynamics of the thermally populated radical with polarization P_{eq}, respectively. The concentrations of the spin equilibrated (C_T) and spin polarized (C_{T^*}) triplet precursor and the time evolution of the escape radical yield ($\phi_{esc}(t)$) are:

$$C_T = (1 - e^{-t/T_1^T})\, e^{-k_q[DQ]t}, \quad (4)$$

$$C_{T^*} = e^{-t/T_1^T}\, e^{-k_q[DQ]t}, \quad (5)$$

$$\phi_{esc}(t) = \phi_{esc}(1 - e^{-k_q[DQ]t}). \quad (6)$$

Thus, the evolution and decay of the FT-EPR signals normalized with the thermal equilibrium intensity is expressed by

$$\frac{M_z(t)}{M_{eq}} = 1 + A\, e^{-t/T_1^R} + B\, e^{-k_q[DQ]t} + C\, e^{-(1/T_1^R + k_q[DQ])t}, \quad (7)$$

where

$$B = \frac{1}{k_q[DQ] - \frac{1}{T_1^R}}\left(\frac{1}{T_1^R} - k_q[DQ]V_d\right), \quad (8)$$

$$C = \frac{k_q[DQ]}{\frac{1}{T_1^R} - \frac{1}{T_1^T} - k_q[DQ]}(V_{dp} - V_d), \quad (9)$$

$$A = -1 - B - C. \quad (10)$$

The intrinsic enhancement factors for the d-TM and the concomitant enhancement factor of the d-TM and p-TM are defined as $V_d = P_d/P_{eq}$ and $V_{dp} = P_{dp}/P_{eq}$, respectively.

The solid lines shown in figure 5 are obtained from the nonlinear least-squares curve fits based on the modified Bloch equation. The enhancement factors obtained for the d-TM (V_d) and for the concomitant d-TM and p-TM (V_{dp}) were 14 and -44 for the present system in 1-PrOH, respectively. The time profiles observed in the different acceptor concentrations are reproduced well using the same data set. This result is strong evidence that the fitting parameters obtained are reasonable. The kinetic parameters and enhancement factors are listed in table 1.

3.3. *Solvent effects*

We measured the echo-FT-EPR spectra to clarify the solvent effects on the intrinsic enhancement factors of the polarization for the present system in several alcoholic solvents. The net-A CIDEP signals due to SOC in the triplet exciplex were also observed in MeOH, EtOH and 1-BuOH. Figure 6 shows the time profiles of the $DQ^{\cdot -}$ central line intensity generated by the photosensitized reduction of DQ (1×10^{-3} mol dm^{-3}) with EY^{2-} (1×10^{-4} mol dm^{-3}) in alcoholic solutions. The measurements were also carried out for DQ concentrations of 4×10^{-3} mol dm^{-3} and 1×10^{-4} mol dm^{-3}. Significant solvent effects on the electron spin polarization and kinetics were observed.

As shown in figure 6, the time profiles observed in MeOH, 1-PrOH, and 1-BuOH were also well reproduced on the basis of the modified Bloch equation. The intrinsic enhancement factors and kinetic parameters are summarized in table 1. The k_q values obtained from an analysis of the buildup of the FT-EPR signals agree well with those determined by the transient absorption experiments. We obtained the V_d values of 8, 11.5 and 16 in MeOH, EtOH, and 1-BuOH, respectively. The V_{dp} value also depends on the solvents.

It is probable that the lifetime of the triplet exciplex is a key factor in determining the enhancement factor of

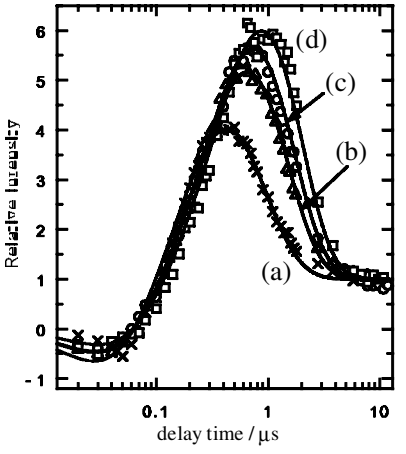

Figure 6. Time profiles of the echo FT-EPR signals ($M_I = 0$) due to $DQ^{\cdot -}$ in the EY^{2-} (1×10^{-4} mol dm^{-3})-DQ (1×10^{-3} mol dm^{-3}) system in MeOH (a), EtOH (b), 1-PrOH (c) and 1-BuOH (d). The solid lines represent nonlinear least-squares curve fits based on the data shown in table 1.

V_d. Both the solvent viscosity and polarity may affect the lifetime of the triplet exciplexes. Therefore, the transient absorption and echo-FT-EPR experiments were performed to examine the solvent polarity effects in ethanol–water mixed solvents. As ethanol is mixed with water, both the viscosity (η) and polarity are remarkably changed. The dielectric constant (ε) monotonically increases with increase in the water mole fraction ($\chi(H_2O)$) while η shows a maximum at about $\chi(H_2O) = 0.8$ [37, 38].

We observed the net-A CIDEP signals of $DQ^{\cdot -}$ in these ethanol–water mixed solvents, indicating that the triplex exciplex has a sufficient lifetime to create the SOC induced polarization in the water containing EtOH solvents. The intrinsic enhancement factors of the CIDEP were determined by the least-squares fits of the time profiles of the FT-EPR signals. The escape radical yield and kinetic parameters were also determined by transient absorption spectroscopy. The values obtained of the kinetic parameters and intrinsic enhancement factors are listed in table 2. Figure 7 also shows plots of V_d versus ε and η. Note that the maximum enhancement factor is obtained in the mixed solvent with the maximum η. The result indicates that the solvent viscosity dominantly affects the enhancement factor V_d as well as the normal triplet mechanism in the present system.

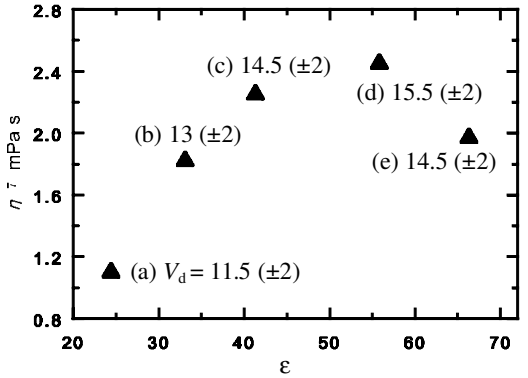

Figure 7. Intrinsic enhancement factors of the d-TM obtained in the EtOH–water mixture solvents: $\chi(H_2O) =$ 0.0 (a), 0.4 (b), 0.6 (c), 0.8 (d), 0.9 (e).

3.4. *Solvent viscosity dependence*

Significant solvent viscosity dependence on the escape radical yield and enhancement factors was observed in the present system. Figure 8 (*a*) plots ϕ_{esc} determined by the transient absorption measurements against the solvent viscosity. The ϕ_{esc} value decreases with increasing η in pure alcohol solvents, indicating that the dissociation rate of the exciplex decreases with increasing viscosity. The external magnetic field (**B**) effects on the ϕ_{esc} were also examined in the present system. The ϕ_{esc} value steeply increased as the **B** increased and then it monotonically decreased. The positive and negative magnetic field effects observed in low and high fields are interpreted in terms of the hyperfine coupling mechanism and the d-TM as well as Δg mechanism, respectively. Thus, the ϕ_{esc} value observed at 340 mT is accidently almost identical to that in zero magnetic field. The

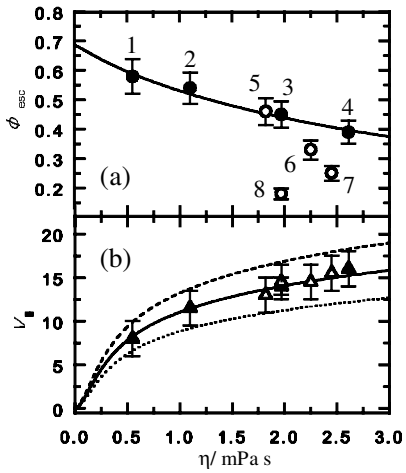

Figure 8. Solvent viscosity dependence of the intrinsic enhancement factors V_d and escape radical yield ϕ_{esc} in alcoholic solvents: MeOH (1), EtOH (2), 1-PrOH (3), 1-BuOH (4) and the EtOH–water mixture solvents of $\chi(H_2O) = 0.4$ (5), 0.6 (6), 0.8 (7), 0.9 (8). The solid lines are the best fits obtained by the calculations based on equations (11) and (17). The lines shown in (*b*) are obtained by calculations using the *D* values of 0.030 cm^{-1} (----), 0.025 cm^{-1} (——), and 0.020 cm^{-1} (·····) of the ZFS parameters in the triplet exciplex.

Table 2. Kinetic parameters and intrinsic enhancement factors of $DQ^{\cdot -}$ generated by the photoinduced electron transfer from EY^{2-} in neat EtOH and EtOH–H_2O mixtures as determined from transient absorption and FT-EPR spectroscopy.

χ_{H_2O} (η/m Pa s; ε)	ϕ_{esc}	$k_q/10^9$ M^{-1} s^{-1}		T_1^T/ns	T_1^R/μs	V_{pd}	V_d
0.0 (1.10; 24.4)	0.54	(3.1)[a]	2.8[b]	10	0.8	−40 (±4)	11.5 (±2)
0.4 (1.82; 33.1)	0.46	(2.9)	2.7	11	1.0	−50 (±4)	13 (±2)
0.6 (2.25; 41.3)	0.33	(2.3)	2.5	11	1.2	−52 (±4)	14.5 (±2)
0.8 (2.45; 55.8)	0.25	(1.9)	2.4	11	1.5	−56 (±4)	15.5 (±2)
0.9 (1.97; 66.3)	0.18	(2.8)	2.6	11	1.7	−50 (±4)	14.5 (±2)

[a] Determined from the transient absorption experiments.
[b] Determined from the FT-EPR experiments.

net-A CIDEP and magnetic field effect observed suggest that the ISC preferentially occurs from the upper sublevels (T_x and T_y) in the triplet exciplex. We assumed the ideal sublevel depopulation in the present work: $k_{isc} = k_{isc}^x = k_{isc}^y$ and $k_{isc}^z = 0$. The dissociation rate is sublevel non-selective: $k_{dis} = k_{dis}^i$ $(i = x, y, z)$.

The dependence of ϕ_{esc} on **B** and η is theoretically expressed by [8]:

$$\phi_{esc}(\mathbf{B}, \eta) = \frac{k_{dis}(k_{dis} + (k_{isc}/3) + 6D_{r,\mathbf{B}})}{(k_{dis} + k_{isc})(k_{dis} + 4D_{r,\mathbf{B}}) + 2k_{dis}D_{r,\mathbf{B}}}, \quad (11)$$

where an effective rotational diffusion constant $D_{r,\mathbf{B}}$ is given by

$$D_{r,\mathbf{B}} = \frac{s(1 - sp_s)}{6sp_s - 2}, \quad (12)$$

with

$$s = 1 + \tfrac{2}{3}k_{isc}, \quad (13)$$

$$p_s = \frac{1}{15}\left\{\frac{5}{s} + \frac{2}{s + 6D_r} + \frac{4(s + 6D_r)}{(s + 6D)^2 + \omega^2} + \frac{4(s + 6D_r)}{(s + 6D_r)^2 + 4\omega^2}\right\}, \quad (14)$$

$$\omega = \frac{g\mu\beta\mathbf{B}}{\eta}. \quad (15)$$

The rotational diffusion constant of the triplet exciplex in zero field D_r is given by

$$D_r = \frac{kT}{8\pi a^3 \eta}, \quad (16)$$

where a is the molecular radius.

The solvent viscosity dependence of V_d was analysed using the analytical expression derived by Serebrennikov and Minaev [39]. In the case of slow spin–lattice relaxation for the triplet exciplex, the expression for P_d as a function of the external magnetic field (**B**) and solvent viscosity is

$$P_d(\mathbf{B}, \eta) = \frac{4\omega k_{dis}(DD_- + 3EE_-)}{45k_0^2k_1^2} \times \left(\frac{1}{1 + (\omega/k_1)^2} + \frac{4}{1 + 4(\omega/k_1)^2}\right), \quad (17)$$

where

$$k_1 = k_0 + 6D_r, \quad (18)$$

$$k_0 = k_{dis} + k_{isc}/3. \quad (19)$$

The zero-field splitting (ZFS) parameters of the triplet exciplex are represented by D and E. The sublevel selective depopulation rates are described by $D_- = (k_{isc}^x + k_{isc}^y)/2 - k_{isc}^z$ and $E_- = (k_{isc}^x + k_{isc}^y)/2$.

The solid lines in figure 8 are obtained by nonlinear curve fits based on equations (11) and (17). Assuming the ideal sublevel back electron tranfer, ZFS values of $d = 0.025\,cm^{-1}$ and $E = 0$, and a molecular radius $a = 0.44\,nm$ for the triplet exciplex, the viscosity dependence of ϕ_{esc} and V_d is reproduced well. We assumed the η dependence of the reaction rate constants: $k_{dis} = (8 \times \eta^{-1}/mPa\,s) \times 10^9\,s^{-1}$ and $k_{isc} = \{(6 \times \eta^{-1}/mPa\,s) + 5\} \times 10^9\,s^{-1}$. There is some uncertainty in the determination of k_{dis} and k_{isc} from the present experiments. A precise analysis of the magnetic field effects on the ϕ_{esc} would be required to determine these reaction constants in high accuracy.

The ϕ_{esc} values decrease with increasing η in pure alcohols and ethanol-rich EtOH–H_2O solvent. In the case of the water-rich mixed solvents, on the other hand, the viscosity dependence of ϕ_{esc} deviates significantly from the plots. This result indicates that the hydrogen bonded network due to water significantly inhibits the escape of the radical from the solvent cage. Note that the η dependence is significantly sensitive to the D value of the ZFS parameters. We obtained a D value of $0.025\,cm^{-1}$ for the triplet exciplex from the curve fits. When we used D values of $0.030\,cm^{-1}$ and $0.020\,cm^{-1}$, the model calculations showed significant deviation from the experimental data, as shown in figure 8 (*b*). The D value obtained is very similar to that of the triplet exciplex of duroquinone and 4-bromodimethylaniline [16].

4. Conclusion

The net-E and A CIDEP of $DQ^{\cdot -}$ observed in the present photoinduced electron transfer reaction suggest clearly the generation of the triplet exciplex or contact radical pair as the reaction intermediate. Coulomb interaction is not important in forming the triplet exciplex, because the EY^{2-}-sensitized reduction system does not form an ion pair by electron transfer. The net-polarized CIDEP is interpreted in terms of heavy atom induced SOC, resulting in the sublevel selective population (p-TM) of the precursor triplet state and the sublevel selective depopulation (d-TM) of the triplet exciplex. The triplet mechanism in the intermediate triplet exciplex provides a good quantitative fit of the solvent viscosity dependence of the radical yield in pure alcohols. On the other hand, in the case of water-rich EtOH–H_2O solvent systems the radical yield deviates remarkably from the plots, suggesting that the hydrogen bonded network due to the water molecules significantly inhibits the escape of radicals from the solvent cage. The ZFS parameters of the triplet exciplex intermediate are estimated

from the viscosity dependence of the intrinsic enhancement factors.

References

[1] Salem, L., and Rowland, C., 1972, *Angew. Chem. Intl Edn Engl.*, **11,** 92.

[2] Steiner, U. E., and Ulrich, T., 1989, *Chem. Rev.*, **89,** 51.

[3] Doubleday, C., Turro, N. J., and Wang, J.-F., 1989, *Accounts chem. Res.*, **22,** 199.

[4] Khudyakov, I. V., Serebrennikov, Y. A., and Turro, N. J., 1993, *Chem. Rev.*, **93,** 537.

[5] Murai, H., Tero-Kubota, S., and Yamauchi, S., 2000, *Electron Spin Resonance*, Vol. 17 (Cambridge: Royal Society of Chemistry) p. 130.

[6] Tero-Kubota, S., Katsuki, A., and Kobori, Y., 2001, *J. Photochem. Photobiol.* C, **2,** 17.

[7] Steiner, U. E., 1981, *Ber. Bunsenges. phys. Chem.*, **85,** 228.

[8] Ulrich, T., Steiner, U. E., and Foll, R. E., 1983, *J. phys. Chem.*, **87,** 1873.

[9] Steiner, U. E., and Haas, W., 1991, *J. phys. Chem.*, **95,** 1880.

[10] Wu, J. Q., Baumann, D., and Steiner, U. E., 1995, *Molec. Phys.*, **84,** 981.

[11] Wolff, H.-J., Burssner, D., and Steiner, U. E., 1995, *Pure appl. Chem.*, **67,** 167.

[12] Katsuki, A. Tero-Kubota, S., and Ikegami, Y., 1993, *Chem. Phys. Lett.*, **209,** 258.

[13] Katsuki, A., Akiyama, K., Ikegami, Y., and Tero-Kubota, S., 1994, *J. Amer. chem. Soc.*, **119,** 12065.

[14] Katsuki, A., Akiyama, K., and Tero-Kubota, S., 1995, *Bull. chem. soc. Jap.*, **68,** 3383.

[15] Sasaki, S., Katsuki, A., Akiyama, K., and Tero-Kubota, S., 1997, *J. Amer. chem. Soc.*, **119,** 1323.

[16] Sasaki, S., Kobori, Y., Akiyama, K., and Tero-Kubota, S., 1998, *J. phys. Chem.* A, **102,** 8078.

[17] Sasaki, S., Kobori, Y., Akiyama, K., and Tero-Kubota, S., 2001, *Res. chem. Intermed.*, **27,** 155.

[18] Katsuki, A., Steiner, U. E., Miliksyants, S., and Paul, H., 1999, *Proceedings of the VIth International Symposium on Magnetic Field and Spin Effects in Chemistry and Related Phenomena*, Emetten, Switzerland, p. 69.

[19] Katsuki, A., Kobori, Y., Tero-Kubota, S., Milikisyants, S., Paul, H., and Steiner, U. E., 2002, *Molec. Phys.*, in press.

[20] Rathore, R., Hubig, S. M., and Kochi, J. K., 1997, *J. Amer. chem. Soc.*, **119,** 11468.

[21] Hubig, S. M., Rathore, R., and Kochi, J. K., 1999, *J. Amer. chem. Soc.*, **121,** 617.

[22] Hubig, S. M., and Kopchi, J. K., 1999, *J. Amer. chem. Soc.*, **121,** 1688.

[23] Adrian, F. J., 1971, *J. chem. Phys.*, **54,** 3918.

[24] Monchick, L., and Adrian, F. J., 1978, *J. chem. Phys.*, **63,** 4376.

[25] Wong, S. K., Hutchison, D. A., and Wan, J. K. S., 1973, *J. chem. Phys.*, **58,** 985.

[26] Atkins, P. W., and Evans, G. T., 1974, *Molec. Phys.*, **27,** 1633.

[27] Savitsky, A. N., Batchelor, S. N., and Paul, H., 1997, *Appl. magn. Reson.*, **13,** 285.

[28] Savitsky, A. N., and Paul, H., 2000, *Chem. Phys. Lett.*, **319,** 403.

[29] Neckers, D. C., and Valdes-Aguilera, O. M., 1993, *Adv. Photochem.*, **18,** 315.

[30] Kasche, V., and Lindqvist, L., 1965, *Photochem. Photobiol.*, **4,** 923.

[31] Kikuchi, K., 1989, *Triplet-Triplet Absorption Spectra* (Tokyo: Bunshin).

[32] Nishimura, Y., Sakuragi, H., and Tokumaru, K., 1992, *Bull. chem. Soc. Jap.*, **65,** 2887.

[33] Islam, S. D.-M., Yoshikawa, Y., Fujitsuka, M., and Ito, O., 1998, *Bull. chem. Soc. Jap.*, **71,** 1543.

[34] Islam, S. D.-M., Konishi, T., Fujitsuka, M., Ito, O., Nakamura, Y., and Usui, Y., 2000, *Photochem. Photobiol.*, **71,** 675.

[35] Misawa, H., Wakisaka, A., Sakuragi, H., and Tokumaru, K., 1985, *Chem. Lett.*, 293.

[36] Patel, K. B., and Willson, R. L., 1973, *J. chem. Soc. Faraday Trans* i, **69,** 814.

[37] Moriyoshi, T., Ishii, T. L., Tamai, Y., and Tado, M., 1990, *J. chem. Eng. Data*, **35,** 17.

[38] Yusa, M., Mather, G. P., and Stager, R. A., 1977, *J. chem. Eng. Data*, **22,** 32.

[39] Serebrennikov, Y. A., and Minaev, B. F., 1987, *Chem. Phys.*, **114,** 359.